Articles

Determination of the Binding Mode of Thienopyrimidinedione Antagonists to the Human Gonadotropin Releasing Hormone Receptor Using Structure−Activity Relationships, Site-Directed Mutagenesis, and Homology Modeling

Stephen F. Betz,*[,†] Francisco M. Lio,[†] Yinghong Gao,[‡] Greg J. Reinhart,[†] Zhiqiang Guo,[‡] Michael F. Mesleh,[‡] Yun-Fei Zhu,[‡] and R. Scott Struthers[†]

Departments of Endocrinology and Medicinal Chemistry, Neurocrine Biosciences, Inc., 12790 El Camino Real, San Diego, California 92130

We have investigated the specific interactions of a series thienopyrimidinediones with the gonadotropin-releasing hormone receptor (GnRH-R). Competitive radioligand binding assays were used to determine the effect of several mutants on nonpeptide binding. Distinct interactions were observed in two separate regions: the N-terminal end of TM7 and the C-terminal end of TM6. The effects of mutants at D302[(7.32)] and H306[(7.36)] suggest that these residues are part of a hydrogen-bond network important for anchoring the nonpeptides. Structure−activity relationships indicated urea substituents on the 6-(4-aminophenyl) group with a trans conformational preference bind with high affinity and are sensitive to D302[(7.32)] mutations. Another interaction area was found between the *N*-benzyl-*N*-methylamino substituent and L300[(6.68)] and Y290[(6.58)]. These interaction sites facilitated the derivation of a model in which a representative member of the series was docked into GnRH-R. The model is consistent with known SAR and illuminates inconsistencies with previous hypotheses regarding how this series interacts with the receptor.

Introduction

Gonadotropin-releasing hormone (GnRH,[a] also known as luteinizing hormone releasing hormone, or LH-RH) is a deca-peptide released by the hypothalamus that stimulates the synthesis and release of the gonadotropins luteinizing hormone and follicle-stimulating hormone.[1] GnRH exerts its actions by binding to and activating the GnRH receptor (GnRH-R) in the pituitary, which belongs to the Class A G-protein-coupled receptor (GPCR) family.[2] Therapeutic strategies, including both peptide agonists and antagonists, have been developed for several clinical indications including prostate cancer, prostate hyperplasia, endometriosis, uterine fibroids, assisted reproductive therapy, and hirsutism.[3−9] Peptide agonist treatment leads to down-regulation of GnRH-R[5,10] and eventually castrates levels of gonadal steroids. One potentially important side effect is an initial exacerbation of symptoms as a result of induced gonado-tropin release.[10,11] Alternatively, treatment with GnRH-R antagonist peptides does not lead to this hormonal "flare".[9,12] While peptide GnRH-R antagonists have been shown to be effective in lowering gonadotropin release, they possess the liability of requiring injection because of poor oral bioavailability (as do GnRH agonist peptides). Accordingly, there is great interest in the development of orally active, nonpeptide GnRH-R antagonists.[13,14]

Several examples of the thienopyrimidinedione class, including **4** (TAK-013, Table 1; also known as sufugolix), have been

shown to be potent and efficacious GnRH antagonists.[15−18] Chronic oral administration of **4** has been shown to suppress serum LH, estradiol, and progesterone levels in female cyno-molgus monkeys,[18] and the compound has reached phase II clinical trials targeting endometriosis. Here, we have adopted a strategy of combining site-directed mutagenesis, compound SAR, and molecular modeling to determine the sites of interaction for this important nonpeptide antagonist series and GnRH-R. Several GPCRs have been studied successfully by this approach by comparing both peptide and nonpeptide ligands, including GnRH-R.[2,19−22] Previously, we had identified over-lapping but nonidentical binding sites for three classes of nonpeptide antagonists of GnRH-R,[22] including a representative thienopyrimidinedione. Here, we sought to determine the specific interactions between that class of nonpeptide antagonists and GnRH-R. Compound SAR, NMR, and mutagenesis pro-vided structure-specific information that was used to produce a model of a representative antagonist bound to the receptor.

Results

Molecule Selection. The nonpeptides tested and their IC$_{50}$ values for wild-type GnRH-R are shown in Table 1. R1 and R2 substitutions were chosen to explore steric, polarity-based, and hydrogen-bonding interactions.

Mutant Selection. Mutant receptors examined here were chosen on the basis of observed interactions between GnRH-R and **4** previously described.[22] In addition, a comparison of these results with unpublished data on the similar compound isopropyl 3-(*N*-benzyl-*N*-methylaminomethyl)-7-(2,6-difluorobenzyl)-4,7-dihydro-2-(4-isobutyrylaminophenyl)-4-oxothieno[2,3-*b*]pyridine-5-carboxylate hydrochloride (T-98475)[2,15] suggested the region including TM6, ECL3, and TM7 to be of critical importance to this class. Figure 1 illustrates a schematic of GnRH-R, high-
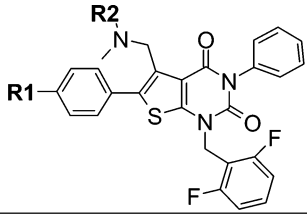
---

* To whom correspondence should be addressed. Phone: 858-617-7893. Fax: 858-617-7696. E-mail: sbetz@neurocrine.com.
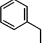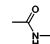 † Department of Endocrinology.
 ‡ Department of Medicinal Chemistry.
 a Abbreviations: GnRH, gonadotropin-releasing hormone; GnRH-R, gonadotropin-releasing hormone receptor; GPCR, G protein-coupled recep-tor; NOE, nuclear Overhauser effect; NOESY, nuclear Overhauser effect spectroscopy; FT, Fourier transform.
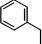
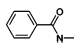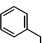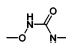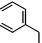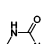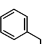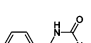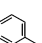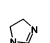**Table 1.** Structures of the Thienopyrimidinedione Series and IC$_{50}$ Affinity Values for the Competition of [^{125}I-His^5,D-Tyr^6]-GnRH versus Wild-Type (F272$^{(6.40)}$L) GnRH-R

Compound	R1	R2	IC$_{50}$ ± Std Dev	Reference
1	H$_2$N—	(benzyl)	210 ± 100	24
2	(formamide)	(benzyl)	29 ± 4	24
3	(benzamide)	(benzyl)	6 ± 3	17
4	(methoxy urea)	(benzyl)	0.8 ± 0.3	17
5	(ethyl urea)	(benzyl)	0.9 ± 0.3	17
6	(benzyl urea)	(benzyl)	20 ± 8	34
7	(cyclic guanidine)	(benzyl)	240 ± 80	34
8	O$_2$N—	(benzyl)	600 ± 100	24
9	O$_2$N—	(phenethyl)	1100 ± 400	24
10	O$_2$N—	(pyridyl ethyl)	52 ± 8	24

lighting the location of mutations selected for this study. Amino acid substitutions for a particular residue were chosen taking into consideration steric bulk and hydrogen-bonding capacity. All GnRH receptors were generated in the F272$^{(6.40)}$L background. The F272$^{(6.40)}$L mutation has been shown to increase cell surface expression of GnRH-R in comparison to the native wild-type receptor without affecting peptide or nonpeptide pharmacology.[22,23] In total, 13 mutants were used for this study, representing 10 different residue positions.

Nonpeptide Binding. The binding affinity of unlabeled [His^5,D-Tyr^6]-GnRH was tested for all of the mutant receptors to assess their pharmacological utility in this study. The IC$_{50}$ values for [His^5,D-Tyr^6]-GnRH for these mutants has been reported,[22] and while some mutant rec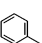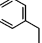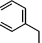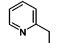eptors exhibited moderate changes in [His^5,D-Tyr^6]-GnRH binding, a comparison of K_i and IC$_{50}$ values for [^{125}I-His^5,D-Tyr^6]-GnRH competition for wild-type and several mutant receptors showed little difference in using K_i or IC$_{50}$ for interpretation purposes. Accordingly, IC$_{50}$-derived values are shown to better compare with previously published results.[22] Table 2 presents the IC$_{50}$ values for each compound as tested against each of the mutant receptors. Figure 2 shows representative radioligand binding curves obtained from the competition between two members of the compound panel and [^{125}I-His^5,D-Tyr^6]-GnRH versus GnRH-R and the D302$^{(7.32)}$A mutant receptor. The effect of a mutation on nonpeptide binding is quantified by calculating the fold-change for that ligand–mutant combination. Fold change is the quotient of the IC$_{50}$ of a ligand for a GnRH-R mutant and the IC$_{50}$ of the same molecule to the wild-type GnRH-R [IC$_{50}$(mutant)/IC$_{50}$(F272$^{(6.40)}$L)]. Table

3 presents the calculated fold-change values of the thieno-pyrimidinedione antagonists versus the GnRH-R mutants.

Specific Interactions in TM7. Previously, D302$^{(7.32)}$ was shown to be involved in the binding of **4**.[22] Here, mutants D302$^{(7.32)}$A and D302$^{(7.32)}$N preferentially affected the binding of each of the urea-substituted compounds (**4**−**6**). The D302$^{(7.32)}$A mutant affected each of the urea-containing molecules by >50-fold, while unsubstituted compounds (**1**, **8**−**10**) or amide-substituted compounds (**2**, **3**) were affected by less than 10-fold. The D302$^{(7.32)}$N mutant had similar effects. We previously hypothesized that D302$^{(7.32)}$ might be a site of interaction of the R1 urea group on **4**.[22] These effects appear to be hydrogen-bond-mediated and more specifically indicate that the γ-urea nitrogen is required to interact with D302$^{(7.32)}$.

Similar to the effects of D302$^{(7.32)}$, mutations at H306$^{(7.36)}$ were also previously shown to affect the binding of **4**.[22] In contrast to the selectivity observed with the urea-containing molecules (**4**−**6**) for D302$^{(7.32)}$ mutations, any compound that contained either an amide or urea moiety was sensitive to mutations at H306$^{(7.36)}$, suggesting that there is a requirement of a carbonyl at the β-position in the R1 substituent of this class of nonpeptides to interact with the histidine side chain. Unsubstituted molecules (**1**, **8**−**10**) showed little sensitivity to mutation, though the nitro-containing molecules were moderately more affected by the H306$^{(7.36)}$E mutation than the H306$^{(7.36)}$A mutation.

Compound **7** was used to test the requirements for both a urea-like HN$_\gamma$ to interact with D302$^{(7.32)}$ and the carbonyl to interact with H306$^{(7.36)}$. As seen in Table 1, the compound has a reduced affinity for the receptor, suggesting that the cyclic guanidine ring is unable to mimic the high-affinity state of the urea-containing compounds. In addition, **7** was less sensitive to mutations at both D302$^{(7.32)}$ and H306$^{(7.36)}$, consistent with this observation. Of note, the binding of the compound is not particularly affected by the H306$^{(7.36)}$E mutation in contrast to the amide and urea-containing compounds, suggesting that the replacement of histidine with an acid-bearing side chain may be better accommodated by the guanidine-containing compound.

On the basis of molecular orbital calculations, Sasaki et al. suggested that **4** favors a urea in the trans orientation because of the potential to form an intramolecular hydrogen bond between the HN$_\alpha$ and the methoxy-O$_\delta$ of the R1 substituent.[17] To further understand the structural basis of the specific interactions between the R1 substituent and the GnRH-R mutants, we undertook experiments to define the conformational preferences of the urea substitutions of the thienopyrimidine-diones. The cis/trans propensity of the urea-containing compounds (**4**−**6**) was examined using two-dimensional nuclear Overhauser effect spectroscopy (NOESY). In these experiments, the spatial proximity of two protons produces a cross-peak in a two-dimensional NMR spectrum connecting the chemical shifts of the two individual protons. The volume of this cross-peak is a quantitative indicator of the time-averaged distance between the two protons in solution—for this system, an index of the urea cis/trans equilibrium. A strong peak is indicative of a favored cis orientation, whereas a weaker (or nonexistent) peak indicates that the protons are predominantly in a trans arrangement. Figure 3 shows the downfield regions of the NOESY spectra of the urea-containing compounds.

For **4**, the cross-peak between the two protons (9.7 and 9.2 ppm) is absent, confirming a stable trans arrangement of the urea, in agreement with the calculations of Sasaki et al.[17] Compound **5** has weak cross-peak volume between the two urea protons, assigned at 8.8 and 6.2 ppm. This suggests a predomi-
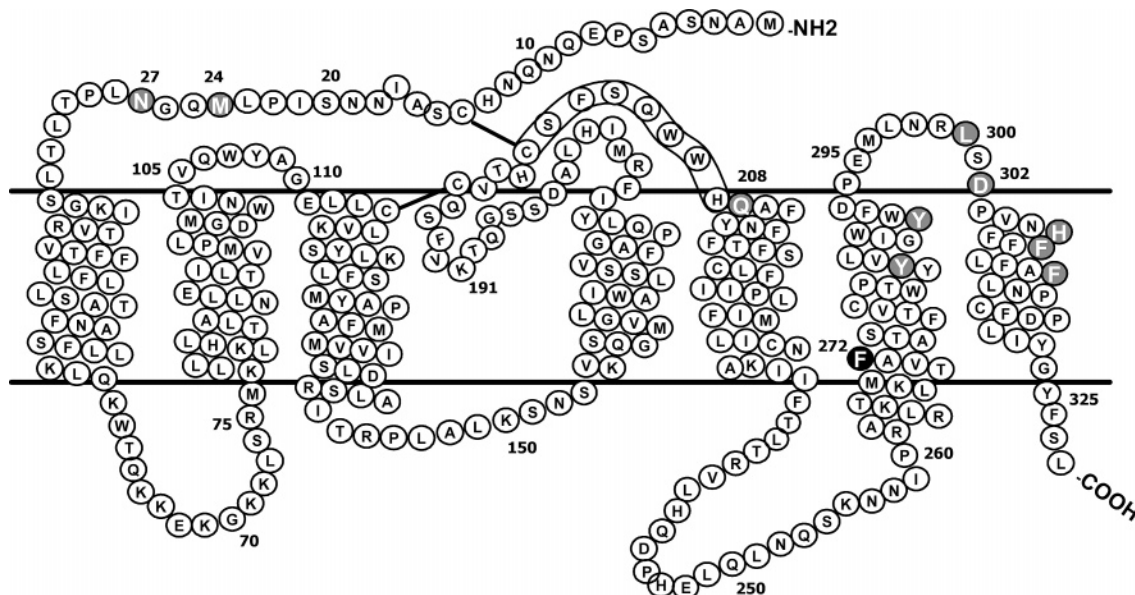
Figure 1. Schematic representation of the primary and predicted secondary structure of human GnRH-R. Residues mutated in the current study are shaded in gray. Predicted α-helical regions are based on the crystallographically determined structure of rhodopsin and are indicated with a 3−4 repeating pattern. F272[(6.40)] (changed to leucine in these experiments) is located at the intracellular edge of transmembrane domain 6 and is shaded black.

Table 2. Antagonist Affinities (IC$_{50}$) and SEM for the Competition of Thienopyrimidinedione Antagonists versus Mutant GnRH-R[a]

	1		2		3		4		5		6		7		8		9		10	
mutant	IC$_{50}$ (nM)	SEM (nM)	IC$_{50}$ (nM)	SEM (nM)	IC$_{50}$ (nM)	SEM (nM)	IC$_{50}$ (nM)	SEM (nM)	IC$_{50}$ (nM)	SEM (nM)	IC$_{50}$ (nM)	SEM (nM)	IC$_{50}$ (nM)	SEM (nM)	IC$_{50}$ (nM)	SEM (nM)	IC$_{50}$ (nM)	SEM (nM)	IC$_{50}$ (nM)	SEM (nM)
F272L	210	100	29	4	6	2	0.8	0.3	0.9	0.3	20	8	240	80	600	100	1100	400	52	8
M24I	4000	1200	2300	450	380	100	110	70	26	6	390	60	*>10000*	nd	*>10000*	nd	*>10000*	nd	*>10000*	nd
N27A	370	100	31	3	26	5	0.7	0.1	1	0.5	30	4	480	30	1600	700	1300	300	200	30
Q208E	1500	900	230	60	31	8	1.2	0.3	1.1	0.1	70	14	1400	800	*>10000*	nd	5000	1000	450	30
Y284L	*>10000*	nd	4400	1800	1500	600	12	3	40	20	6000	3000	5000	2000	*>10000*	nd	*>10000*	nd	2000	200
Y290L	390	230	52	5	20	3	0.5	0.2	0.31	0.05	70	30	350	60	1100	200	1900	800	900	200
L300A	1600	600	240	50	22	9	1.9	0.4	2.1	0.2	190	40	1020	90	*>10000*	nd	*>10000*	nd	110	10
D302A	390	76	210	90	15	8	190	80	60	20	1100	200	3300	900	1900	700	1600	700	58	8
D302N	530	160	160	30	13	4	120	30	50	10	500	100	2100	100	1400	500	1900	500	40	7
H306A	710	110	1700	500	400	90	24	5	40	10	600	300	4400	800	3000	1000	3300	700	240	40
H306E	500	100	1600	700	800	300	100	20	60	30	4000	1000	800	300	*>10000*	nd	7100	100	400	100
F309L	950	90	1100	400	100	40	6	1	9	3	900	300	1800	500	*>10000*	nd	*>10000*	nd	2650	70
F309Q	*>10000*	nd	2400	1000	220	50	10	2	28	9	1200	400	5200	400	*>10000*	nd	*>10000*	nd	3600	300
F313L	*>10000*	nd	2000	400	400	100	24	7	23	4	1400	500	*>10000*	nd	*>10000*	nd	*>10000*	nd	4500	400

[a] IC$_{50}$ values are an average of at least three experiments. Binding experiments that did not produce a full-binding curve were estimated to have IC$_{50}$ > 10 µM and are shown in italics. All mutants listed are in the F272[(6.40)]L background. The IC$_{50}$ values for F272[(6.40)]L are listed in the top row for reference.

nantly trans conformation, albeit with a greater cis population than **4**. Interestingly, **6** (benzyl-substituted urea) has a significant cross-peak between the protons at 8.9 and 6.8 ppm, indicating that **6** more prefers a cis conformation. To quantitate these results, the volumes of these cross-peaks were compared to the volumes of other cross-peaks between fixed atoms that can be used as a "ruler". The volumes of NOEs relating two protons are proportional to the inverse sixth power of the distance between the two protons. Average interproton distances are calculated using the expression

$$r^6 = 2.5^6 \left(\frac{\text{volume of reference crosspeak}}{\text{volume of urea crosspeak}} \right)$$

Assuming an interproton distance of 2.5 Å for adjacent protons on an aromatic ring, the average interproton distances are calculated to be 4.4, 3.4, and 2.9 Å for **4**, **5**, and **6**, respectively. Those values are consistent with the range of interproton distances derived from calculations performed on simple model compounds. Compound **7** was also examined because the cyclic guanidine ring essentially ensures that the

two urea-like protons will be in a cis conformation. Rather than a urea side chain, this compound contains a cyclic guanidine ring. The NMR results show that this structure is in fact tautomeric, with strong cross-peaks reflecting exchange between the two conformations on the NMR time scale (data not shown).

Specific Interactions in TM6. The nitro-substituted compounds at R1 were synthesized to optimize the requirements at R2 in the absence of specific interactions near TM7.[24] With a benzyl or ethylphenyl substitution, these compounds are of rather low affinity for GnRH-R (Table 1). An ethyl-2-pyridyl substitution at R2 results in over a 10-fold increase in affinity. Although **8** and **9** are not particularly robust probes of structure−function in this series because of their low affinity for the wild-type receptor, the nitro compounds **8**−**10** exhibit sensitivity to mutations much like the other members of the series (Table 3). They are strongly affected by mutations at M24, Y284[(6.52)], and the aromatics in TM7 (F309[(7.39)], F313[(7.43)]). These compounds show no specific interactions, unlike the R1-substituted compounds, to D302[(7.32)] or H306[(7.36)] mutations in TM7, though the set shows moderate loss of affinity across each member to
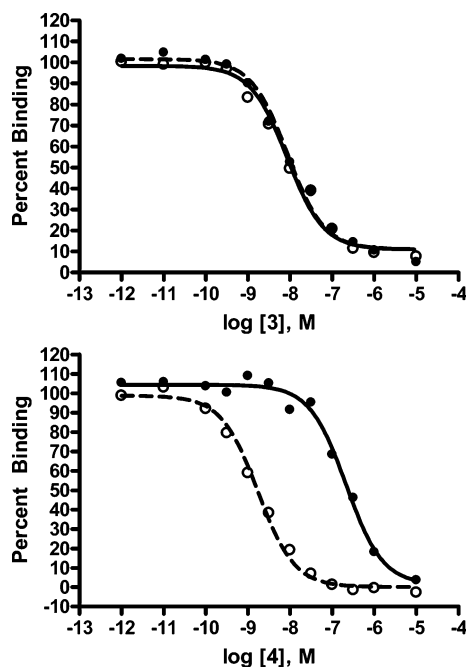
Figure 2. Competition binding of [^{125}I-His^5,D-Tyr^6] by different antagonists to wild-type and D302$^{(7.32)}$A GnRH-R: (○) wild-type GnRH-R; (●) D302$^{(7.32)}$A GnRH-R.

the changes at H306$^{(7.36)}$. The only mutations to produce differences within the set are L300$^{(6.68)}$A and Y290$^{(6.58)}$ (Table 3). The binding of **8** and **9** is eliminated by the L300$^{(6.68)}$A mutant, whereas the affinity of **10** is essentially unaffected. Reciprocally, the binding of the pyridyl-containing compound **10** is affected 17-fold by the Y290$^{(6.58)}$L mutant, while the affinities of the phenyl-compounds **8** and **9** are not. This suggests that there is a conformational shift in the binding mode of the R2 substituent depending on the nature of the aromatic substitution; namely, the phenyl-containing compounds are interacting with L300$^{(6.68)}$, while the pyridyl-containing compound shifts to interact with the nearby Y290$^{(6.58)}$. These residues are modeled to be in proximity of one another (see ref 22 and Figure 4a below), and the reorientation of **10** toward the side chain Y290$^{(6.58)}$ can be easily accommodated. This potential interaction is reasonable, and the tendency of pyridyl-containing ligands to interact with tyrosine(s) has been observed in crystal structures of soluble proteins.[25–27]

Discussion

Specific and Class Interactions. A comparison of the NMR, binding affinity and mutagenesis data (Tables 2 and 3) indicates that for the thienopyrimidinedione class of GnRH-R antagonists high-affinity binding to the receptor can be mediated through a *trans*-urea at the R1 site and that sensitivity to mutations at D302$^{(7.32)}$ is correlated with affinity. Moreover, affinity and sensitivity to mutation at D302$^{(7.32)}$ are also related to *trans*-urea stability. The R1 site also requires the presence of a β-carbonyl for moderate affinity (see Table 1). Through mutagenesis and SAR, the sites on the receptor responsible for the binding of this class have been identified as D302$^{(7.32)}$ and H306$^{(7.36)}$, respectively. For the R2 site, compounds **8–10** have shown a "toggle" between L300$^{(6.68)}$ and Y290$^{(6.58)}$ depending on the identity of the substituent.

Several other mutant receptors were examined to understand their effect on the binding of the thienopyrimidinedione antagonists. There are other residues where mutations affect binding, including Y284$^{(6.52)}$, F309$^{(7.39)}$, and F313$^{(7.43)}$. The

results for this series are shown in Tables 2 and 3 and are consistent with previous results reported for **4**. None of these other residues exhibit a clear chemical structure-dependent sensitivity to mutation in the same way as D302$^{(7.32)}$/H306$^{(7.36)}$ and Y290$^{(6.58)}$/L300$^{(6.68)}$. This suggests that these residues, while important for interactions between these nonpeptide antagonists and the receptor, do not occur at regions where this series has been varied.

Ligand Bound Model. The combination of certain residues that affect the binding of the series as a class and others that show evidence of reciprocal SAR between the compound and the receptor structure facilitated the derivation of a docked model of **4** bound to the receptor, shown in Figure 4. As shown in Figure 4a, the compound is bound across the transmembrane binding pocket. The R2 substituent is located in proximity to L300$^{(6.68)}$, though it is clear that simple rotations would allow the pyridyl-substituted **10** to interact predominantly with Y290$^{(6.58)}$. The difluorobenzyl ring is inserted into the aromatic pocket adjacent to Y284$^{(6.52)}$. The remaining phenyl ring is in proximity to Q208$^{(5.35)}$, although direct interaction seems unlikely here, and this is consistent with the moderate effects observed (Table 3). That phenyl ring is likely closest to Y211$^{(5.38)}$. Direct assessment of this residue and its interactions may be difficult, however, because the Y211$^{(5.38)}$A mutant has been reported not to express.[28]

The R1 substituent **4** interacts with both D302$^{(7.32)}$ and H306$^{(7.36)}$, and its proposed interactions are highlighted in Figure 4b. Specifically indicated are the hydrogen bonds between D302$^{(7.32)}$O$_\delta$ and the HN$_\gamma$ of the R1 substituent and that between imidazole proton of H306$^{(7.36)}$ and the urea carbonyl of **4**. Heavy atom to heavy atom distances are estimated to be within the range accepted for hydrogen bonds (2.7 and 3.7 Å, respectively). The longer distance of the H306$^{(7.36)}$-mediated hydrogen bond raises the possibility that this interaction could be water-mediated, but these methods and this model cannot discriminate between those possibilities. The most straightforward solution is presented in Figure 4b.

There are two residues listed in Table 3 for which an explanation of their effects on the binding of the thieno-pyrimidinediones is not straightforward. Replacement of M24 in the N-terminal domain has a generalized and large effect on the binding of this class of molecules, consistent with previous observations of **4**.[22] It is likely that this residue participates in a substructure required for high-affinity binding (perhaps in conjunction with one or more of the extracellular loops[22]) and that changing it affects the class as a whole. The F313$^{(7.43)}$L mutation also affects every member of the nonpeptide panel and has previously been shown to be responsible for species-selective binding to a series of quinolone GnRH-R antagonists.[29] The model presented in Figure 4a does not suggest that this residue is in proximity to the molecule. We hypothesize that F313$^{(7.43)}$ is involved in internal aryl–aryl stacking with F309$^{(7.39)}$. F309$^{(7.39)}$ is in very close proximity to the phenyl group that bridges the core to the R1 substituent. Exchange of F313$^{(7.43)}$ destabilizes the intramolecular aryl–aryl interaction, resulting in losses of affinity that are very similar to those of the destabilizing F309$^{(7.39)}$Q mutation.

Nonpeptide–Peptide Interaction Comparison. We and others have previously proposed that certain features of the thienopyrimidinedione class of GnRH antagonists mimic individual residues of the GnRH peptide.[15,24] Notably, the methyl-amine mimics Arg^8 in GnRH and interacts with D302$^{(7.32)30,31}$ and the phenyl group that bridges the core and the R1 substituent mimics Tyr^5 in GnRH, which has been hypothesized to interact

Table 3. Fold Change Values for the Competition of Thienopyrimidinedione Antagonists versus Mutant GnRH-R[a]

		Compound									
mutant	location	1	2	3	4	5	6	7	8	9	10
		General and Nonspecific Effects									
M24I	N-term	**19**	**79**	**63**	**138**	**29**	**20**	***>40***	***>16***	*>9*	***>190***
N27A	N-term	1.8	1.1	4.3	0.9	1.1	1.5	2.0	2.7	1.2	3.8
Q208E	5.35	7.1	7.9	5.2	1.5	1.2	3.5	5.8	***>16***	4.5	8.7
Y284L	6.52	***>45***	**150**	**250**	**15**	**44**	**300**	**21**	***>16***	*>9*	**38**
F309L	7.39	4.5	**38**	**17**	7.5	**10**	**45**	7.5	***>16***	*>9*	**51**
F309Q	7.39	***>45***	**83**	**37**	**12**	**31**	**60**	**22**	***>16***	*>9*	**69**
F313L	7.43	***>45***	**69**	**67**	**30**	**26**	**70**	***>40***	***>16***	*>9*	**86**
		Specific TM6 Effects									
L300A	6.68/ECL3	7.6	8.3	3.7	2.4	2.3	9.5	4.3	***>16***	*>9*	2.1
Y290L	6.58	1.9	1.8	3.3	0.6	0.3	3.5	1.5	1.8	1.7	**17**
		Specific TM7 Effects									
D302A	7.32/ECL3	1.9	7.2	2.5	**238**	**67**	**55**	**14**	3.2	1.5	1.1
D302N	7.32/ECL3	2.5	5.5	2.2	**150**	**56**	**25**	8.8	2.3	1.7	0.8
H306A	7.36	3.4	**59**	**67**	**30**	**44**	**30**	**18**	5.0	3.0	4.6
H306E	7.36	2.4	**55**	**133**	**125**	**67**	**200**	3.3	***>16***	6.5	7.7

[a] Thienopyrimidinedione antagonists exhibit structure-specific sensitivity to GnRH-R mutants. Location refers to the position of the residue in the schematic in Figure 1. "N-term" refers to the extracellular N-terminal extension preceding the transmembrane region. Fold-change values are defined as [IC$_{50}$(mutant)/IC$_{50}$(F272$^{(6.40)}$L)]. Fold change values greater than 10 are shown in **bold**. Fold change values estimated from IC$_{50}$ values of ">10 μM" are indicated in ***bold italics***.
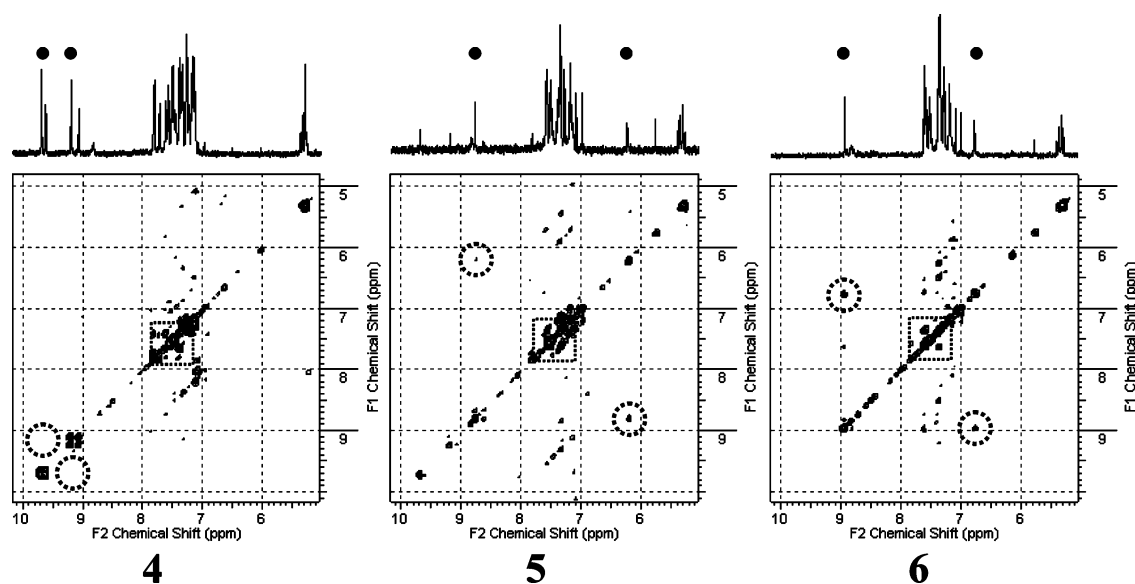

Figure 3. NMR spectra of urea-containing compounds (**4**−**6**). Upper spectra show 1D ^{1}H NMR of each compound, and urea protons are indicated with black circles (●). The lower spectra show the 2D ^{1}H NMR NOESY spectra of each compound. The predicted locations of the NOE cross-peaks between the two urea protons are indicated by dashed circles.

with Y290$^{(6.58)}$.[2,22,32] The results presented here are consistent with a nearly inverted orientation. As shown in Figure 4b, we hypothesize that the R1 substituent interacts primarily with D302$^{(7.32)}$ and H306$^{(7.36)}$. The data here strongly suggest that this interaction is hydrogen-bonding in nature and does not mimic the charged-based interactions of Arg^8 with D302$^{(7.32)}$. The observation that the R1 substituent is the center of sensitivity to mutation at D302$^{(7.32)}$ and the lack of any structure-based effects at the aminomethyl or R2 substituents rules out that the methylamine is a counterion to D302$^{(7.32)}$. The interactions of the R2 substituent are dependent on its identity, but the compounds studied here (**8**−**10**) interact with either L300$^{(6.68)}$ or Y290$^{(6.58)}$, corresponding most closely with the interactions of Tyr^5 in GnRH, though this is a comparison of interactions of nonpeptide antagonists bound to the inactive state of the receptor to peptide agonists interacting with the receptor's activated state. The model presented in Figure 4 is a representation of the inactive state and does not take into account any movements of the receptor upon activation.

In summary, we have used mutagenesis data, coupled with compound SAR and molecular modeling, to define the binding mode of an important class of nonpeptide GnRH-R antagonists. This model can lead to structure-guided development of new molecules with greater affinity and/or selectivity as well as hypothesis-driven investigations into ligand−receptor structure and function. By comparing the binding of this class of antagonists to other important series,[13,14] we can begin to unravel the specific interactions that guide ligand binding to this receptor, ultimately with the goal of determining how specific binding events govern downstream biological activities.

Experimental Section

Nomenclature. A GnRH peptide is named by the residue's three-letter abbreviation, its sequence position in the peptide superscripted (e.g., His^5 denotes a His substitution at position 5 of the GnRH peptide). Receptor residues are named by Ballesteros−Weinstein numbering method,[33] using a residue's one-letter abbreviation and primary sequence position, with the superscripted characters
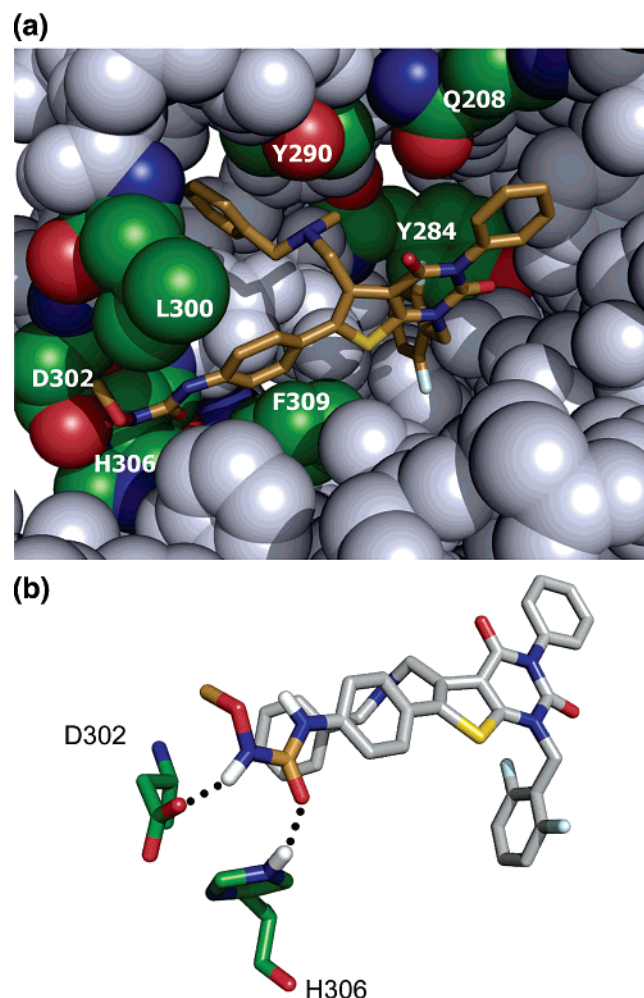
(a)

(b)

Figure 4. Homology model of human GnRH-R with **4** bound. (a) Shown is the antagonist within the receptor binding pocket. Residues examined in this study are colored by atom type. The remainder of the receptor is shown in gray. The Ballesteros−Weinstein labeling for each of these residues has also been omitted for clarity. (b) Specific hydrogen-bonding interactions between the R1 substituent of **4** and the side chains of D302[(7.32)] and H306[(7.36)] are shown. Putative hydrogen bonds are represented as dotted lines.

representing its transmembrane helix and number position within that helix based on its position relative to the most evolutionarily conserved residue in that helix (e.g., F272[(6.40)]). GnRH-R mutants are denoted by wild-type residue, residue number, and mutant residue, (e.g., D302[(7.32)]A denotes an aspartic acid to alanine mutation at position 302). Residues in the N-terminal extension have no annotation.

Nonpeptide Antagonist Synthesis. The compounds displayed in Table 1 were all synthesized using previously described methods[17,24,34] (see Table 1).

Mutagenesis. GnRH-R was cloned and expressed as described previously.[20,21] Site-directed mutants were generated using the QuikChange site-directed mutagenesis kit (Stratagene). The GnRH-R cDNA was cloned into the expression vector pcDNA3.1(+). The complete coding region for each mutant receptor was confirmed by DNA sequence analysis (ABI Prism 377 DNA sequencer, Applied Biosystems Inc., Foster City, CA).

Cell Culture and Transient Transfections. Cell culture reagents were purchased from Cellgro (Fisher Scientific, Tustin, CA). COS-7 cells were from American Type Cell Culture (Manassas, VA) and were cultured in Dulbeccos's modified Eagle's medium (DMEM, MediaTech Inc., Hemdon, VA) supplemented with 10% fetal bovine serum, 10 mM HEPES, 2 mM L-glutamine, 1 mM sodium pyruvate, 50 U/mL penicillin, and 50 μg/mL streptomycin. Cells were transfected in a phosphate buffered saline (PBS) cocktail containing

5×10^7 cells and 50 μg of GnRH-R DNA construct using a BTX ElectroCell manipulator ECM 600 (Fischer Scientific, Pittsburgh, PA) applying 1000 μF capacitance, 48 Ω resistance, and 300 V/cm charging voltage.

Membrane Preparation. COS-7 cells were harvested, washed, and resuspended in membrane buffer (20 mM HEPES, pH 7.2, 6 mM MgCl$_2$, 1 mM EDTA) 36−48 h after transfection. Cells were lysed by release of pressure at 900 psi in a nitrogen chamber after a 30-min incubation at 4 °C. Nuclei and other cellular debris were removed by centrifugation at 1000 rpm for 10 min at 4 °C. The membrane fraction was collected by centrifugation at 16 500 rpm for 45 min at 4 °C and subsequently resuspended in membrane buffer at a concentration of 1 mg/mL. Membrane preparations were aliquoted, frozen in liquid nitrogen, and stored at −80 °C until they were needed.

Competition Binding Assays. Radioligand binding assays were performed in 96-well filter plates (Multiscreen 1.2 μm glass-fiber plates, Millipore, Bedford, MA). Each assay point consisted of a 100 μL cocktail of cell membrane containing the mutant GnRH-R of interest (5−40 μg), 300 pM [^{125}I-His^5,D-Tyr^6]-GnRH, and varying concentrations of small molecule, all prepared in assay buffer (10 mM HEPES, pH 7.45, 150 mM NaCl, 0.1% bovine serum albumin (fraction V)). Assay plates were shaken at 100 rpm for 2 h at room temperature and then vacuum-filtered. The filter plates were washed twice with PBS and then dried completely. Scintillation fluid (Scint20, Packard Instruments, Downers Grove, IL) was added to each well prior to detection in a TopCount NXT counter (Packard Instruments, Downers Grove, IL).

Data Analysis. Experiments were performed using 12 points per experiment. IC$_{50}$ values were calculated using the "one-site competition" nonlinear regression analysis of Prism (GraphPad, version 4.01, San Diego, CA). Compounds with IC$_{50}$ values estimated to be greater than the highest concentration used (10 μM) for this study were assigned the arbitrary value of ">10 μM". Each experiment was performed at least three times.

NMR Spectroscopy. Studies of the cis/trans conformation of compounds were conducted using 2D nuclear Overhauser effect spectroscopy (NOESY) on a Bruker Avance 500 MHz spectrometer equipped with an inverse SEI-probe and z-axis gradients. Because of limiting aqueous solubility, all samples were prepared by diluting a 10 mM DMSO stock solution to 1 mM in DMSO-d_6, with 5% (v/v) ^{1}H$_2$O added in order to observe exchangeable urea protons. The spectral width of the 2D NOESY experiments was 5000 Hz in both dimensions, with 1024 × 512 complex points being acquired, multiplied by a sinbell, and zero-filled to 2048 points in both dimensions prior to FT. The mixing time for these experiments was set to 600 ms. Assignments of the urea resonances were made by adding ^{2}H$_2$O to the DMSO solution and monitoring the disappearance of the exchangeable protons. Results were confirmed by the multiplicities of the protons adjacent to methylene groups (triplets) and compared well to those obtained by simulation.

Molecular Modeling. The model of GnRH-R was built as previously described.[22] Diverse docking poses with varied conformations of **4** within the binding site were generated using the MMFF94x force field implemented in MOE (Chemical Computing Group, Montreal, Canada).[35,36] The receptor was rigid and **4** was allowed to be flexible. Approximately 1800 diverse docking solutions were generated. These poses were evaluated for solutions that were consistent with the experimental mutagenesis constraints. For example, 182 docking solutions with a distance between the urea and D302[(7.32)] of less than 6 Å were retained. Redundant solutions were removed by filtering those with pairwise distance rmsd less than 1 Å to yield 48 potential docking modes of **4**. Ten diverse solutions consistent with the ligand being close to other known areas of contact (i.e., S118[(3.29)22], F309[(7.39)], L300[(6.68)]) were then selected from the remaining docking modes for further investigation. Molecular dynamics (MD) simulation was carried out using MOE with weakly constrained 7TM backbone atoms (tether weight of 5) and more weakly constrained conserved residue side chains (tether weight of 1) with the MMFF94x force field at 400 K for 75 ps followed by simulated annealing at 300, 200, and

100 K and minimization. The entire system (excluding the exterior lipid-spanning region) was then solvated with explicit water. The whole system was minimized with all atoms fixed except water hydrogen followed by a 5 ps MD run at 400 K and minimization to reorient the water hydrogens. All water atoms were then unfixed and equilibrated with another 5 ps MD trajectory at 400 K.

A wall function was applied to the water molecules (weight of 20) to prevent them from "escaping" during simulation. The entire system was minimized with the above-mentioned tether weights to an rms gradient of <1. MD simulation of the whole was then carried out as before at 400 K for 100 ps followed by simulated annealing at 300, 200, and 100 K and minimization. Finally, all atoms in the system other than 7TM backbone atoms were allowed to move freely for another 50 ps at 400 K before simulated annealing and minimization to produce the final ligand-bound model.

References

(1) Fink, G. Gonadotropin secretion and its control. *The Physiology of Reproduction*; Raven Press: New York, 1988; pp 1349−1377.

(2) Millar, R. P.; Lu, Z. L.; Pawson, A. J.; Flanagan, C. A.; Morgan, K.; et al. Gonadotropin-releasing hormone receptors. *Endocr. Rev.* **2004**, *25*, 235−275.

(3) Lunenfeld, B. *GnRH Analogues: The State of the Art at the Millennium*; The Parthenon Publishing Group: New York, 1999.

(4) Barbieri, R. L. Hormone treatment of endometriosis: the estrogen threshold hypothesis. *Am. J. Obstet. Gynecol.* **1992**, *166*, 740−745.

(5) Conn, P. M.; Crowley, W. F., Jr. Gonadotropin-releasing hormone and its analogs. *Annu. Rev. Med.* **1994**, *45*, 391−405.

(6) Emons, G.; Schally, A. V. The use of leutenizing releasing hormone agonists and antagonists in gynaecological cancers. *Hum. Reprod.* **1994**, *9*, 1364−1379.

(7) Millar, R. P.; Zhu, Y.-F.; Chen, C.; Struthers, R. S. Progress towards the development of non-peptide orally-active gonadotropin-releasing hormone (GnRH) antagonists: Therapeutic implications. *Br. Med. Bull.* **2000**, *56*, 761−772.

(8) Grundker, C.; Emons, G. Role of gonadotropin-releasing hormone (GnRH) in ovarian cancer. *Reprod. Biol. Endocrinol.* **2003**, *1*, 65.

(9) Herbst, K. L. Gonadotropin-releasing hormone antagonists. *Curr. Opin. Pharmacol.* **2003**, *3*, 660−666.

(10) Kiesel, L. A.; Rody, A.; Greb, R. R.; Szilagi, A. Clinical use of GnRH analogs. *Clin. Endocrinol.* **2002**, *56*, 677−687.

(11) Goulet, M. T. Gonadotropin releasing hormone antagonists. *Annu. Rep. Med. Chem.* **1995**, *30*, 169−178.

(12) Coccia, M. E.; Comparetto, C.; Bracco, G. L.; Scarselli, G. GnRH antagonists. *Eur. J. Obstet. Gynecol. Reprod. Biol.* **2004**, *1158*, S44−S56.

(13) Armer, R. E.; Smelt, K. H. Non-peptidic GnRH receptor antagonists. *Curr. Med. Chem.* **2004**, *11*, 3017−3028.

(14) Zhu, Y. F.; Chen, C.; Struthers, R. S. Nonpeptide gonadotropin releasing hormone antagonists. *Annu. Rep. Med. Chem.* **2004**, *39*, 99−110.

(15) Cho, N.; Harada, M.; Imaeda, T.; Imada, T.; Matsumoto, H.; et al. Discovery of a novel, potent, and orally active nonpeptide antagonist of the human luteinizing hormone-releasing hormone (LHRH) receptor. *J. Med. Chem.* **1998**, *41*, 4190−4195.

(16) Sasaki, S.; Imaeda, T.; Hayase, Y.; Shimizu, Y.; Kasai, S.; et al. A new class of potent nonpeptide luteinizing hormone-releasing hormone (LHRH) antagonists: design and synthesis of 2-phenylimidazo-[1,2-*a*]pyrimidin-5-ones. *Bioorg. Med. Chem. Lett.* **2002**, *12*, 2073−2077.

(17) Sasaki, S.; Cho, N.; Nara, Y.; Harada, M.; Endo, S.; et al. Discovery of a thieno[2,3-*d*]pyrimidine-2,4-dione bearing a *p*-methoxyureido-phenyl moiety at the 6-position: a highly potent and orally bioavailable non-peptide antagonist for the human luteinizing hormone-releasing hormone receptor. *J. Med. Chem.* **2003**, *46*, 113−124.

(18) Hara, T.; Araki, H.; Kusaka, M.; Harada, M.; Cho, N.; et al. Suppression of pituitary−ovarian axis by chronic oral administration of a novel nonpeptide gonadotropin-releasing hormone antagonist, TAK-013, in cynomolgus monkeys. *J. Clin. Endocrinol. Metab.* **2003**, *88*, 1697−1704.

(19) Kristiansen, K. Molecular mechanisms of ligand binding, signaling and regulation within the superfamily of G-protein-coupled receptors: molecular modeling and mutagenesis approaches to receptor structure and function. *Pharmacol. Ther.* **2004**, *103*, 21−80.

(20) Ott, T. R.; Troskie, B. E.; Roeske, R. W.; Illing, N.; Flanagan, C. A.; et al. Two mutations in extracellular loop 2 of the human GnRH receptor convert an antagonist to an agonist. *Mol. Endocrinol.* **2002**, *16*, 1079−1088.

(21) Reinhart, G. J.; Xie, Q.; Liu, X. J.; Zhu, Y. F.; Fan, J.; et al. Species selectivity of nonpeptide antagonists of the gonadotropin-releasing hormone receptor is determined by residues in extracellular loops II and III and the amino terminus. *J. Biol. Chem.* **2004**, *279*, 34115−34122.

(22) Betz, S. F.; Reinhart, G. J.; Lio, F. M.; Chen, C.; Struthers, R. S. Overlapping, nonidentical binding sites of different classes of nonpeptide antagonists for the human gonadotropin-releasing hormone receptor. *J. Med. Chem.* **2006**, *49*, 637−347.

(23) Flanagan, C. A.; Fromme, B. J.; Davidson, J. S.; Millar, R. P. A high affinity gonadotropin-releasing hormone (GnRH) tracer, radio-iodinated at position 6, facilitates analysis of mutant GnRH receptors. *Endocrinology* **1998**, *139*, 4115−4119.

(24) Guo, Z.; Chen, Y.; Wu, D.; Zhu, Y. F.; Struthers, R. S.; et al. Synthesis and structure−activity relationships of thieno[2,3-*d*]pyrimidine-2,4-dione derivatives as potent GnRH receptor antagonists. *Bioorg. Med. Chem. Lett.* **2003**, *13*, 3617−3622.

(25) Li, M.; Dyda, F.; Benhar, I.; Pastan, I.; Davies, D. R. The crystal structure of *Pseudomonas aeruginosa* exotoxin domain III with nicotinamide and AMP: Conformational differences with the intact exotoxin. *Proc. Natl. Acad. Sci. U.S.A.* **1995**, *92*, 9308−9312.

(26) Orville, A. M.; Lipscomb, J. D.; Ohlendorf, D. H. Crystal Structure of substrate and substrate analog complexes of protocatechuate 3,4-dioxygenase: endogenous Fe^{3+} ligand displacement in response to substrate binding. *Biochemistry* **1997**, *36*, 10052−10066.

(27) Korman, T. P.; Hill, J. A.; Vu, T. N.; Tsai, S.-C. Structural analysis of actinorhodin polyketide ketoreductase: cofactor binding and substrate specificity. *Biochemistry* **2004**, *43*, 14529−14538.

(28) Hoffmann, S. H.; ter Laak, T. T.; Kuhne, R.; Reilander, H.; Beckers, T. Residues within transmembrane helices 2 and 5 of the human gonadotropin-releasing hormone receptor contribute to agonist and antagonist binding. *Mol. Endocrinol.* **2000**, *14*, 1099−1115.

(29) Cui, J.; Smith, R. G.; Mount, G. R.; Lo, J. L.; Yu, J.; et al. Identification of Phe313 of the gonadotropin-releasing hormone (GnRH) receptor as a site critical for the binding of nonpeptide GnRH antagonists. *Mol. Endocrinol.* **2000**, *14*, 671−681.

(30) Flanagan, C. A.; Becker, I. I.; Davidson, J. S.; Wakefield, I. K.; Zhou, W.; et al. Glutamate 301 of the mouse gonadotropin-releasing hormone receptor confers specificity for arginine 8 of mammalian gonadotropin-releasing hormone. *J. Biol. Chem.* **1994**, *269*, 22636−22641.

(31) Fromme, B. J.; Katz, A. A.; Roeske, R. W.; Millar, R. P.; Flanagan, C. A. Role of aspartate 7.32 (302) of the human gonadotropin-releasing hormone receptor in stabilizing a high affinity ligand conformation. *Mol. Pharmacol.* **2001**, *60*, 1280−1287.

(32) Hovelmann, S.; Hoffmann, S. H.; Kuhne, R.; ter Laak, T. T.; Reilander, H.; et al. Impact of aromatic residues within transmembrane helix 6 of the human gonadotropin-releasing hormone receptor upon agonist and antagonist binding. *Biochemistry* **2002**, *41*, 1129−1136.

(33) Ballasteros, J.; Weinstein, H. Integrated methods for the construction of three-dimensional models and computational probing of structure−function relations in G-protein coupled receptors. *Methods Neurosci.* **1995**, *25*, 366−428.

(34) Compounds **6** and **7** were synthesized according to the methods described in ref 24.

(35) Halgren, T. A. MMFF VI. MMFF94s option for energy minimization studies. *J. Comput. Chem.* **1999**, *20*, 720−729.

(36) Halgren, T. A. MMFF VII. Characterization of MMFF94, MMFF94s, and other widely available force fields for conformational energies and for intermolecular-interaction energies and geometries. *J. Comput. Chem.* **1999**, *20*, 730−748.